

## High-resolution XANES study of $\text{Eu}(\text{Ba}_{1-x}\text{R}_x)_2\text{Cu}_3\text{O}_{7+\delta}$ (R = Eu, Pr)

This content has been downloaded from IOPscience. Please scroll down to see the full text.

2006 New J. Phys. 8 215

(<http://iopscience.iop.org/1367-2630/8/9/215>)

View [the table of contents for this issue](#), or go to the [journal homepage](#) for more

Download details:

IP Address: 140.113.38.11

This content was downloaded on 26/04/2014 at 08:41

Please note that [terms and conditions apply](#).

## High-resolution XANES study of $\text{Eu}(\text{Ba}_{1-x}\text{R}_x)_2\text{Cu}_3\text{O}_{7+\delta}$ ( $\text{R} = \text{Eu}, \text{Pr}$ )

J M Chen<sup>1,5</sup>, R S Liu<sup>2,5</sup>, J M Lee<sup>1,3</sup>, K T Lu<sup>1</sup>, T J Yang<sup>3</sup>,  
M J Kramer<sup>4</sup> and R W McCallum<sup>4</sup>

<sup>1</sup> National Synchrotron Radiation Research Center (NSRRC),  
Hsinchu, Taiwan, Republic of China

<sup>2</sup> Department of Chemistry, National Taiwan University, Taipei,  
Taiwan, Republic of China

<sup>3</sup> Department of Electrophysics, National Chiao Tung University,  
Hsinchu, Taiwan, Republic of China

<sup>4</sup> Ames Laboratory, US Department of Energy, Iowa State University,  
Ames, IA 50011, USA

E-mail: [jmchen@nsrrc.org.tw](mailto:jmchen@nsrrc.org.tw) and [rslu@ntu.edu.tw](mailto:rslu@ntu.edu.tw)

*New Journal of Physics* **8** (2006) 215

Received 10 May 2006

Published 27 September 2006

Online at <http://www.njp.org/>

doi:10.1088/1367-2630/8/9/215

**Abstract.** We have probed the distribution of hole carriers in  $\text{Eu}(\text{Ba}_{1-x}\text{Eu}_x)_2\text{Cu}_3\text{O}_{7+\delta}$  ( $x = 0-0.2$ ) and  $\text{Eu}(\text{Ba}_{1-x}\text{Pr}_x)_2\text{Cu}_3\text{O}_{7+\delta}$  ( $x = 0-0.25$ ) by O K-edge and Cu L-edge x-ray absorption spectra. Upon Eu and Pr substitution at the Ba site in  $\text{Eu}(\text{Ba}_{1-x}\text{R}_x)_2\text{Cu}_3\text{O}_{7+\delta}$ , the concentration of holes in the  $\text{CuO}_2$  planes becomes greatly diminished. The depletion rate of hole carriers within the  $\text{CuO}_2$  planes in  $\text{Eu}(\text{Ba}_{1-x}\text{Pr}_x)_2\text{Cu}_3\text{O}_{7+\delta}$  is greater than that in  $\text{Eu}(\text{Ba}_{1-x}\text{Eu}_x)_2\text{Cu}_3\text{O}_{7+\delta}$ . The rate of  $T_c$  suppression with Pr doping in  $\text{Eu}(\text{Ba}_{1-x}\text{Pr}_x)_2\text{Cu}_3\text{O}_{7+\delta}$  is accordingly greater than that in  $\text{Eu}(\text{Ba}_{1-x}\text{Eu}_x)_2\text{Cu}_3\text{O}_{7+\delta}$ .

<sup>5</sup> Authors to whom any correspondence should be addressed.

**Contents**

<b>1. Introduction</b>	<b>2</b>
<b>2. Experiments</b>	<b>3</b>
<b>3. Results and discussion</b>	<b>3</b>
<b>4. Conclusion</b>	<b>8</b>
<b>Acknowledgments</b>	<b>8</b>
<b>References</b>	<b>8</b>

**1. Introduction**

Replacing yttrium in  $\text{YBa}_2\text{Cu}_3\text{O}_7$  with other rare-earth elements, apart from Pr [1, 2], neither affects its superconducting properties nor significantly alters the corresponding superconducting transition temperature ( $T_c$ ). In  $\text{Y}_{1-x}\text{Pr}_x\text{Ba}_2\text{Cu}_3\text{O}_7$ ,  $T_c$  decreases monotonically with increasing Pr doping, and superconductivity becomes completely quenched for a proportion of Pr greater than 0.55 [1]. This suppression of superconductivity of  $\text{R}_{1-x}\text{Pr}_x\text{Ba}_2\text{Cu}_3\text{O}_7$  due to Pr doping has been a controversial topic in the field of high- $T_c$  cuprates.

In  $\text{R}_{1-x}\text{Ba}_{2-x}\text{Cu}_3\text{O}_{7+\delta}$ , the light rare-earth elements R (La, Pr, Nd, Sm, Eu and Gd) are known to occupy both the Ba site and the rare-earth site. If  $\text{R}^{3+}$  has an ionic radius approaching that of  $\text{Ba}^{2+}$ , it is amenable to a high degree of substitution of R for Ba without phase separation [3]–[5]. In  $\text{Nd}_{1+x}\text{Ba}_{2-x}\text{Cu}_3\text{O}_{7+\delta}$ , the existence of a solid solution has been found in a range from  $x = 0$  to 0.8 [3]. The substitution of  $\text{R}^{3+}$  ion at the  $\text{Ba}^{2+}$  site is accompanied with a change in the crystal structure from orthorhombic to tetragonal. For example, in  $\text{Eu}(\text{Ba}_{1-x}\text{R}_x)_2\text{Cu}_3\text{O}_{7+\delta}$  (R = Eu, Pr, and La), the space group is  $\text{P}_{\text{mmm}}$ , thus orthorhombic, for  $x < 0.15$ , whereas the structure collapses to a tetragonal space group,  $\text{P}_{4/\text{mmm}}$ , for  $x = 0.15$ . When  $\text{R}^{3+}$  occupies the  $\text{Ba}^{2+}$  site in  $\text{Eu}(\text{Ba}_{1-x}\text{R}_x)_2\text{Cu}_3\text{O}_{7+\delta}$ , neutron-diffraction data show that the extra oxygen is incorporated in fully oxygenated orthorhombic structure and occupies the anti-chain Cu–O(5) sites [5]. As the Cu–O chain acts as a charge reservoir, the extra oxygen alters the distribution of holes in the structure.

The chemical substitution of a  $\text{R}^{3+}$  ion for a  $\text{Ba}^{2+}$  ion in  $\text{Eu}(\text{Ba}_{1-x}\text{R}_x)_2\text{Cu}_3\text{O}_{7+\delta}$  leads to a monotonically decreasing superconducting temperature. The suppression of superconductivity has, however, no simple relation to the ionic size of  $\text{R}^{3+}$  substitutes [5, 6]. Moreover, the change in superconductivity is indirectly related to structural distortion. Especially noteworthy is that Pr doping in  $\text{Eu}(\text{Ba}_{1-x}\text{R}_x)_2\text{Cu}_3\text{O}_{7+\delta}$  and  $\text{Nd}(\text{Ba}_{1-x}\text{R}_x)_2\text{Cu}_3\text{O}_{7+\delta}$  suppresses superconductivity more effectively than other light rare-earth substitutions [5, 6]. Several mechanisms have been proposed to explain this more rapid depression of superconductivity by Pr in  $\text{Eu}(\text{Ba}_{1-x}\text{R}_x)_2\text{Cu}_3\text{O}_{7+\delta}$ , and  $\text{Nd}(\text{Ba}_{1-x}\text{R}_x)_2\text{Cu}_3\text{O}_{7+\delta}$ , including ionic size, magnetic pair breaking, Pr 4f hybridization or crystal-field effects [5]. With regard to this suppression of superconductivity, it is therefore of interest to elucidate whether Pr has a unique electronic characteristic among the light rare-earth elements. This question has become increasingly crucial because superconductivity of  $\text{PrBa}_2\text{Cu}_3\text{O}_7$  is reported in some crystals, thin films, and polycrystalline materials [7]–[9]. The absence or occurrence of superconductivity in  $\text{PrBa}_2\text{Cu}_3\text{O}_7$  has re-opened the field for discussion.

The aim of this study was to investigate the effect of substitution by various rare-earth elements at the Ba sites, and in particular to clarify the distinction between the behaviour of

Pr and other light rare-earth elements. We measured systematically the variation of unoccupied electronic structure near the Fermi level for compounds in the series  $\text{Eu}(\text{Ba}_{1-x}\text{R}_x)_2\text{Cu}_3\text{O}_{7+\delta}$  ( $\text{R} = \text{Eu}, \text{Pr}$ ). Although Xu *et al* [5] reported the physical properties of  $\text{Eu}(\text{Ba}_{1-x}\text{R}_x)_2\text{Cu}_3\text{O}_{7+\delta}$ , the relationship between the hole distribution and superconductivity properties is not established in detail. Hole states are known to play a pivotal role for superconductivity in *p*-type cuprate superconductors [10]. In this study, we measured O K-edge and Cu L-edge x-ray absorption near-edge structure (XANES) spectra of  $\text{Eu}(\text{Ba}_{1-x}\text{R}_x)_2\text{Cu}_3\text{O}_{7+\delta}$  ( $\text{R} = \text{Eu}, \text{Pr}$ ) to discover how the variation of the hole distribution near the Fermi level is related to the superconducting properties.

## 2. Experiments

Detailed procedures for the preparation of  $\text{Eu}(\text{Ba}_{1-x}\text{R}_x)_2\text{Cu}_3\text{O}_{7+\delta}$  ( $\text{R} = \text{Eu}, \text{Pr}$ ) were reported elsewhere [5]. In brief, polycrystalline  $\text{Eu}(\text{Ba}_{1-x}\text{R}_x)_2\text{Cu}_3\text{O}_{7+\delta}$  ( $\text{R} = \text{Eu}, \text{Pr}$ ) samples were synthesized by the standard solid-state reaction method using dried rare-earth oxides,  $\text{BaCO}_3$ , and  $\text{CuO}$ . The copper oxide was heated in oxygen at  $800^\circ\text{C}$  to achieve complete oxidation. The initial grinding of the oxides and carbonate was performed in a micromill in order to reduce the particle size and speed the diffusion process. The powder was then calcined several times in  $\text{CO}_2$ -free air for 24–48 h, with intermediate grinding. The calcination steps were repeated until x-ray diffraction (XRD) and differential thermal analysis (DTA) confirmed the formation of a single-phase solid solution. The calcined samples were then annealed in 100% oxygen atmosphere at a temperature near the melting temperature of the solid solution. Oxygenation of the samples was performed on powders at  $450^\circ\text{C}$  for 24 h with a slow cool to room temperature.

X-ray absorption measurements were performed at the 6 m high-energy spherical grating monochromator beamline of the National Synchrotron Radiation Research Center in Taiwan. X-ray absorption spectra were recorded in the x-ray fluorescence yield mode with a microchannel plate detector. In contrast to the electron-yield measurement, the measurement of x-ray fluorescence yield is sensitive to the bulk of a sample with a probing depth of thousands of angstroms. The photon energies were calibrated using the known O K-edge and Cu L-edge absorption peaks of  $\text{CuO}$ . The energy resolution of the monochromator was set to approx. 0.15 eV for the O K-edge energy region and approx. 0.3 eV for the Cu L-edge energy region.

## 3. Results and discussion

Figure 1 shows O K-edge x-ray absorption spectra of  $\text{Eu}(\text{Ba}_{1-x}\text{Eu}_x)_2\text{Cu}_3\text{O}_{7+\delta}$  for  $x = 0$ –0.2. The principal features of the O K-edge x-ray absorption spectrum for samples with  $x = 0$  are two distinct pre-edge lines at approx. 528.3 and 529.3 eV with a shoulder at approx. 527.6 eV, and a broad line at approx. 537 eV. The low-energy pre-edge peaks with energies less than 532 eV are ascribed to excitations of O 1s-core electrons to hole states with predominantly 2p character on the oxygen sites. The features at energies above 532 eV are attributed to continuum absorption to empty d states or f states of Eu, Ba 4d, Cu 4s or Cu 4p states hybridized with O 2p states [11]. We found that the O K-edge x-ray absorption spectra above 550 eV of  $\text{Eu}(\text{Ba}_{1-x}\text{Eu}_x)_2\text{Cu}_3\text{O}_{7+\delta}$ , which are likely dominated by the contribution from multiple scattering effects, are quite similar and nearly independent of Eu substitution. Accordingly, the O K-edge absorption spectra in

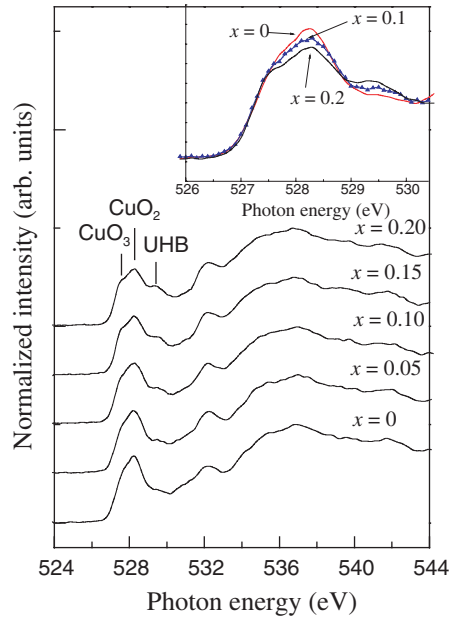


**Figure 1.** O K-edge x-ray absorption spectra of  $\text{Eu}(\text{Ba}_{1-x}\text{Eu}_x)_2\text{Cu}_3\text{O}_{7+\delta}$  for  $x = 0-0.2$ .

figure 1 for various compounds with varied  $x$  were normalized to have the same integrated area in the range 550–560 eV.

The  $\text{Eu}(\text{Ba}_{1-x}\text{Eu}_x)_2\text{Cu}_3\text{O}_{7+\delta}$  compounds for  $x < 0.15$  are isomorphic with orthorhombic  $\text{YBa}_2\text{Cu}_3\text{O}_{7-\delta}$ . With increased Eu content in  $\text{Eu}(\text{Ba}_{1-x}\text{Eu}_x)_2\text{Cu}_3\text{O}_{7+\delta}$  for  $x \geq 0.15$ , the compounds become tetragonal for fully oxygenated samples. This tetragonal structure is isomorphic with  $\text{YBa}_2\text{Cu}_3\text{O}_{6.4}$ . As shown in figure 1, the O K-edge x-ray absorption spectrum of  $\text{Eu}(\text{Ba}_{1-x}\text{Eu}_x)_2\text{Cu}_3\text{O}_{7+\delta}$  for  $x = 0$  exhibits features similar to that observed for  $\text{YBa}_2\text{Cu}_3\text{O}_{7-\delta}$  with  $\delta = 0$  [12]. We therefore adopt the same scheme as for  $\text{YBa}_2\text{Cu}_3\text{O}_{7-\delta}$  in assigning the present O 1s absorption spectra of  $\text{Eu}(\text{Ba}_{1-x}\text{Eu}_x)_2\text{Cu}_3\text{O}_{7+\delta}$ . The pre-edge feature at approx. 528.3 eV is attributed to excitations of O 1s electrons to O 2p holes in the  $\text{CuO}_2$  planes, i.e., Zhang–Rice (ZR) states [11, 13]. The pre-edge peaks at approx. 527.6 eV in figure 1 are due to superposition of O 2p hole states in the apical oxygen sites and CuO chains [14]. The absorption peak at approx. 529.3 eV is assigned to a transition  $3d^{10}L \rightarrow O1s^{-1}3d^{10}$ , i.e., into O 2p states hybridized with the upper Hubbard band (UHB) with predominantly Cu 3d character. This pre-edge structure results from the hybridization in the ground state of the Cu  $3d^9$  and Cu  $3d^{10}L$  configurations, in which L denotes ligand holes in the O 2p orbitals. Due to the strong on-site correlation effects on the copper sites in the cuprate superconductors, the UHB state has always been assumed to exist.

As is discernible in the inset of figure 1, the spectral weight of the pre-edge feature at approx. 528.3 eV originating from O 2p hole states in the  $\text{CuO}_2$  planes is greatly diminished with increasing concentration of Eu, whereas the UHB intensity becomes significantly enhanced concurrently. This change is consistent with the known transfer of spectral weight from the hole states in the  $\text{CuO}_2$  planes to the UHB due to strong correlation effects in the  $\text{CuO}_2$  planes, as observed in O 1s absorption spectra of other hole-doped cuprate superconductors [15, 16]. This behaviour provides clear evidence in support of the filling of O 2p holes in the  $\text{CuO}_2$  planes by chemical substitution of  $\text{Eu}^{3+}$  for  $\text{Ba}^{2+}$  in  $\text{Eu}(\text{Ba}_{1-x}\text{Eu}_x)_2\text{Cu}_3\text{O}_{7+\delta}$ . In contrast, hole carriers in the  $\text{CuO}_3$  ribbons show a minor change with Eu substitution.

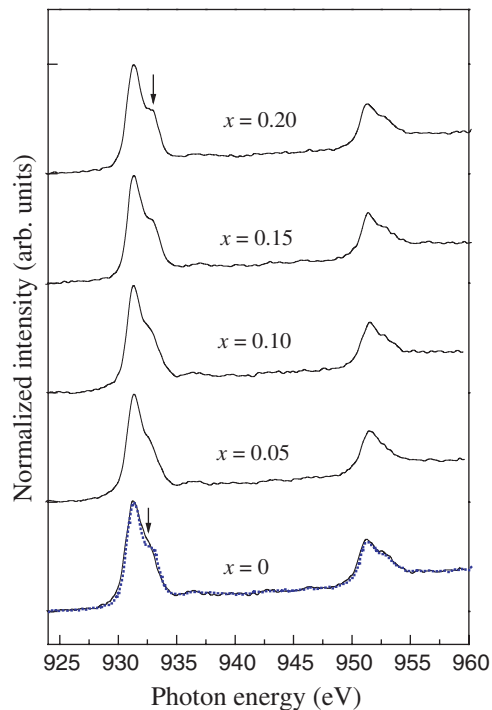


**Figure 2.** Cu L-edge x-ray absorption spectra of  $\text{Eu}(\text{Ba}_{1-x}\text{Eu}_x)_2\text{Cu}_3\text{O}_{7+\delta}$  for  $x = 0$ – $0.2$ . For comparison, the Cu L-edge x-ray absorption spectrum of the  $x = 0.2$  sample is plotted as a dashed curve.

Figure 2 reproduces the Cu  $L_{23}$ -edge x-ray absorption spectra of  $\text{Eu}(\text{Ba}_{1-x}\text{Eu}_x)_2\text{Cu}_3\text{O}_{7+\delta}$  for  $x = 0$ – $0.2$  in the energy range 925–960 eV. For samples with  $x = 0$ , the Cu  $L_3$ -edge absorption spectrum is asymmetric with a tail extending to greater energies, and can be decomposed into two features at approx. 931.2 and 932.6 eV, respectively. The spectral shape of the Cu  $L_3$  absorption edge for samples with  $x = 0$  resembles that of single-crystalline  $\text{YBa}_2\text{Cu}_3\text{O}_{7-\delta}$  for  $E \parallel ab$  plane [17]. For a sample with  $x = 0.2$ , apart from an absorption feature at approx. 931.2 eV, a more pronounced shoulder at approx. 932.9 eV is discernible, as indicated by arrowheads in figure 2. The samples with  $x = 0.2$  show spectral features of the Cu  $L_3$  absorption edge similar to single-crystalline  $\text{YBa}_2\text{Cu}_3\text{O}_{7-\delta}$  for  $E \parallel c$  axis. The shoulders shift to greater energy approx. 0.3 eV for samples with Eu doping increasing from  $x = 0$  to 0.2.

The absorption features at approx. 931.2 and 951.2 eV shown in figure 2 are ascribed to transitions from  $\text{Cu}(2p_{3/2,1/2})3d^9\text{-O}2p^6$  ground states to  $\text{Cu}(2p_{3/2,1/2})^{-1}3d^{10}\text{-O}2p^6$  excited states, in which  $(2p_{3/2,1/2})^{-1}$  represents a  $2p_{3/2}$  or  $2p_{1/2}$  hole, i.e., being due to  $\text{Cu}^{\text{II}}$  [17]. The high-energy shoulders are assigned to transitions from the  $\text{Cu}(2p_{3/2,1/2})3d^9\text{L}$  ground state to the  $\text{Cu}(2p_{3/2,1/2})^{-1}3d^{10}\text{L}$  excited state, in which L denotes the O 2p ligand holes, i.e., being due to  $\text{Cu}^{\text{III}}$ . The spectral weight of the high-energy shoulder therefore corresponds to the total concentration of holes in the  $\text{CuO}_2$  planes and the  $\text{CuO}_3$  chains. We ascribe the shoulder at approx. 932.6 and 932.9 eV to transitions predominantly into hole states in the  $\text{CuO}_2$  planes and the  $\text{CuO}_3$  chains, respectively [18]. The energy shift in figure 2 for samples from  $x = 0$  to 0.2 might reflect the fact that holes located in the squares of the  $\text{CuO}_3$  chains produce an energy shift larger than for the more delocalized holes in the  $\text{CuO}_2$  planes. It is clear from figure 2 that

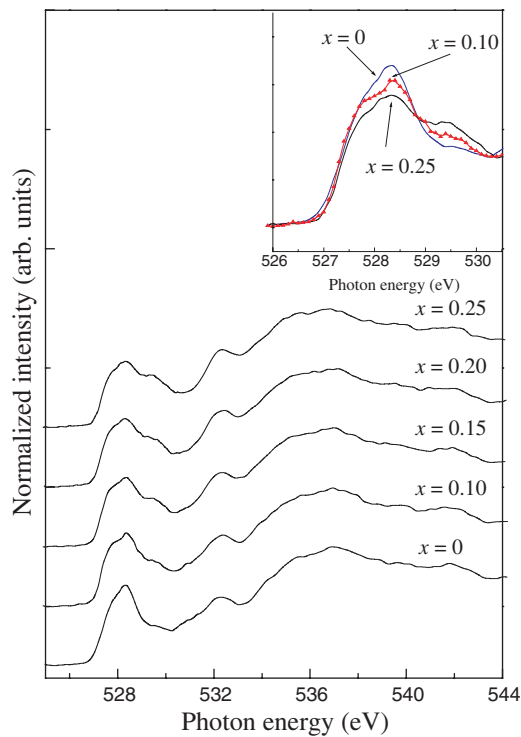


**Figure 3.** O K-edge x-ray absorption spectra of  $\text{Eu}(\text{Ba}_{1-x}\text{Pr}_x)_2\text{Cu}_3\text{O}_{7+\delta}$  for  $x = 0-0.25$ .

the spectral weight of high-energy shoulder at approx. 932.6 eV is diminished as a result of the Eu doping, corresponding to less holes in the  $\text{CuO}_2$  planes. In contrast, the intensity of shoulder at approx. 932.9 eV is slightly increased with Eu doping, indicating slight more holes in the  $\text{CuO}_3$  ribbons. Based on the neutron diffraction studies in  $\text{Eu}(\text{Ba}_{1-x}\text{Eu}_x)_2\text{Cu}_3\text{O}_{7+\delta}$ , the total O content increases as a result of the Eu doping [5]. In a fully oxygenated orthorhombic structure, the extra oxygen occupies the anti-chain Cu–O(5) sites. The extra oxygen thus leads to a slight increase of hole concentration in the  $\text{CuO}_3$  ribbons [18]. The results derived from the Cu L-edge absorption spectra are consistent with those from the O K-edge spectra of  $\text{Eu}(\text{Ba}_{1-x}\text{Eu}_x)_2\text{Cu}_3\text{O}_{7+\delta}$  in figure 1.

Figure 3 shows O K-edge x-ray absorption spectra of the  $\text{Eu}(\text{Ba}_{1-x}\text{Pr}_x)_2\text{Cu}_3\text{O}_{7+\delta}$  compounds for  $x = 0-0.25$ . As noted, the O K-edge x-ray absorption spectra of  $\text{Eu}(\text{Ba}_{1-x}\text{Pr}_x)_2\text{Cu}_3\text{O}_{7+\delta}$  exhibit features similar to those observed for  $\text{Eu}(\text{Ba}_{1-x}\text{Eu}_x)_2\text{Cu}_3\text{O}_{7+\delta}$ . Based on the accumulated knowledge on various high-temperature copper-oxide phases [11, 13], [19]–[22], we therefore adopt the same assignment scheme discussed above for the O 1s x-ray absorption spectra of  $\text{Eu}(\text{Ba}_{1-x}\text{Pr}_x)_2\text{Cu}_3\text{O}_{7+\delta}$ . Near the O 1s edge, pre-edge peaks at approx. 527.6 and 528.3 eV in figure 3 are assigned to transitions into O 2p holes located in the  $\text{CuO}_3$  ribbons and the  $\text{CuO}_2$  planes, respectively. The absorption feature at approx. 529.3 eV originates from the UHB. As shown in the inset of figure 3, the concentration of holes in the  $\text{CuO}_2$  planes becomes decreased, whereas the UHB intensity is concurrently increased, with increasing concentration of dopant Pr in  $\text{Eu}(\text{Ba}_{1-x}\text{Pr}_x)_2\text{Cu}_3\text{O}_{7+\delta}$ .

We compare the depletion rate of hole carriers due to Eu and Pr doping in  $\text{Eu}(\text{Ba}_{1-x}\text{Eu}_x)_2\text{Cu}_3\text{O}_{7+\delta}$  and  $\text{Eu}(\text{Ba}_{1-x}\text{Pr}_x)_2\text{Cu}_3\text{O}_{7+\delta}$ , respectively. In figure 4, the pre-edge

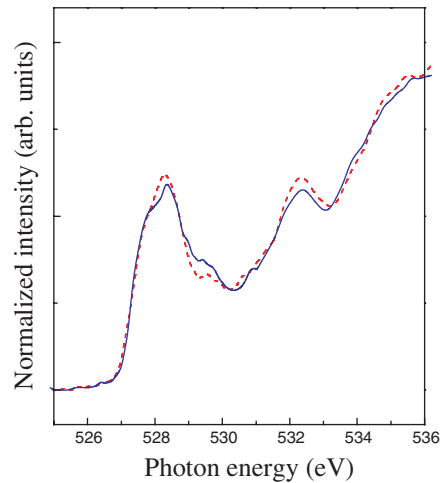


**Figure 4.** O K-edge x-ray absorption pre-edge spectra of  $\text{Eu}(\text{Ba}_{1-x}\text{Eu}_x)_2\text{Cu}_3\text{O}_{7+\delta}$  for  $x = 0.1$  (dash line) and  $\text{Eu}(\text{Ba}_{1-x}\text{Pr}_x)_2\text{Cu}_3\text{O}_{7+\delta}$  for  $x = 0.1$  (solid line).

region of O 1s x-ray absorption spectra of  $\text{Eu}(\text{Ba}_{1-x}\text{Eu}_x)_2\text{Cu}_3\text{O}_{7+\delta}$  for  $x = 0.1$  and of  $\text{Eu}(\text{Ba}_{1-x}\text{Pr}_x)_2\text{Cu}_3\text{O}_{7+\delta}$  for  $x = 0.1$  are displayed as a representative example. The O K-edge absorption spectra in figure 4 are normalized to the integrated area between 550 and 560 eV with respect to the number of O atoms per unit cell, providing absolute intensities of the pre-edge features for the  $\text{Eu}(\text{Ba}_{1-x}\text{Eu}_x)_2\text{Cu}_3\text{O}_{7+\delta}$  and  $\text{Eu}(\text{Ba}_{1-x}\text{Pr}_x)_2\text{Cu}_3\text{O}_{7+\delta}$  compounds. The reason is that the spectra above 550 eV for  $\text{Eu}(\text{Ba}_{1-x}\text{Eu}_x)_2\text{Cu}_3\text{O}_{7+\delta}$  and  $\text{Eu}(\text{Ba}_{1-x}\text{Pr}_x)_2\text{Cu}_3\text{O}_{7+\delta}$  are similar nearly independent of the varied oxygen environments (not shown).

As shown in figure 4, the spectral weights of the pre-edge features at approx. 527.6 eV are nearly identical for both compounds. Therefore, the average number of hole carriers in the  $\text{CuO}_3$  chains is approximately the same for both compounds. In contrast, the hole carriers within the  $\text{CuO}_2$  planes in  $\text{Eu}(\text{Ba}_{1-x}\text{Pr}_x)_2\text{Cu}_3\text{O}_{7+\delta}$  for  $x = 0.1$  are fewer than in  $\text{Eu}(\text{Ba}_{1-x}\text{Eu}_x)_2\text{Cu}_3\text{O}_{7+\delta}$  for  $x = 0.1$ . Moreover, the spectral weight of the UHB in  $\text{Eu}(\text{Ba}_{1-x}\text{Pr}_x)_2\text{Cu}_3\text{O}_{7+\delta}$  for  $x = 0.1$  is greater than that in  $\text{Eu}(\text{Ba}_{1-x}\text{Eu}_x)_2\text{Cu}_3\text{O}_{7+\delta}$  for  $x = 0.1$ . The UHB is known to be strongly correlated with the hole states in the  $\text{CuO}_2$  planes. This result thus confirms that the hole concentration in the  $\text{CuO}_2$  planes in  $\text{Eu}(\text{Ba}_{1-x}\text{Pr}_x)_2\text{Cu}_3\text{O}_{7+\delta}$  is less than that in  $\text{Eu}(\text{Ba}_{1-x}\text{Eu}_x)_2\text{Cu}_3\text{O}_{7+\delta}$ . As well established, the concentration of holes in the  $\text{CuO}_2$  planes is strongly correlated with  $T_c$  [23]. The rate of  $T_c$  suppression in  $\text{Eu}(\text{Ba}_{1-x}\text{Pr}_x)_2\text{Cu}_3\text{O}_{7+\delta}$  with Pr doping is thus expected in principle to be faster than that in  $\text{Eu}(\text{Ba}_{1-x}\text{Eu}_x)_2\text{Cu}_3\text{O}_{7+\delta}$  with Eu substitution, which is indeed the case.

When Pr is incorporated into the  $(\text{Eu},\text{Pr})(\text{Ba},\text{Pr})_2\text{Cu}_3\text{O}_{7+\delta}$  structure, it can occupy either the rare-earth site or the barium site [24]. Because  $\text{Eu}^{3+}$  has an ionic radius 0.950 Å significantly smaller than that of  $\text{Pr}^{3+}$  1.013 Å, Pr is expected to have a greater tendency to substitute for Ba rather than for Eu. However, substitution of Pr at the rare-earth site in  $\text{Eu}(\text{Ba}_{1-x}\text{Pr}_x)_2\text{Cu}_3\text{O}_{7+\delta}$  is proposed to be not negligible. Moreover, the rate of  $T_c$  suppression for Pr occupying the rare-earth site in  $(\text{Eu}_{1-x}\text{Pr}_x)\text{Ba}_2\text{Cu}_3\text{O}_{7+\delta}$  is greater than that for Pr occupying the Ba site in  $\text{Eu}(\text{Ba}_{1-x}\text{Pr}_x)_2\text{Cu}_3\text{O}_{7+\delta}$  with the same proportion of Pr [24]. The  $T_c$  suppression of  $(\text{R}_{1-x}\text{Pr}_x)\text{Ba}_2\text{Cu}_3\text{O}_7$  with Pr doping has been demonstrated to be due to the hole depletion effect arising from the existence of  $\text{Pr } 4f_{z(x^2-y^2)}\text{-O } 2p_\pi$  hybridized states proposed by Fehrenbacher and



Rice (FR) [14, 19]. The rapid depression of  $T_c$  upon Pr doping in  $\text{Eu}(\text{Ba}_{1-x}\text{Pr}_x)_2\text{Cu}_3\text{O}_{7+\delta}$  might accordingly be due to partial substitution of Pr at the rare-earth site, whereas Pr at the Ba site might behave similarly to other light rare-earth elements [6].

#### 4. Conclusion

From analysis of O K-edge and Cu L-edge x-ray absorption spectra, we have derived the distribution of hole states at the various oxygen sites in  $\text{Eu}(\text{Ba}_{1-x}\text{Eu}_x)_2\text{Cu}_3\text{O}_{7+\delta}$  ( $x = 0-0.2$ ) and  $\text{Eu}(\text{Ba}_{1-x}\text{Pr}_x)_2\text{Cu}_3\text{O}_{7+\delta}$  ( $x = 0-0.25$ ). Upon substitution of Eu and Pr at the Ba site in  $\text{Eu}(\text{Ba}_{1-x}\text{R}_x)_2\text{Cu}_3\text{O}_{7+\delta}$ , the hole concentration in the  $\text{CuO}_2$  planes is greatly diminished. The high-energy shoulders in the Cu  $L_{23}$ -edge absorption spectra of  $\text{Eu}(\text{Ba}_{1-x}\text{Eu}_x)_2\text{Cu}_3\text{O}_{7+\delta}$  arise from  $\text{Cu}3d^9L$  defected states to  $\text{Cu}2p^{-1}3d^{10}L$  excited states, here L denotes the ligand holes in the  $\text{CuO}_3$  chains and the  $\text{CuO}_2$  planes. With increasing Eu doping in  $\text{Eu}(\text{Ba}_{1-x}\text{Eu}_x)_2\text{Cu}_3\text{O}_{7+\delta}$ , the shoulders shift to greater energy approx. 0.3 eV from  $x = 0$  to 0.2. The spectral weight of high-energy shoulder at approx. 932.6 eV is diminished as a result of the Eu doping, corresponding to less holes in the  $\text{CuO}_2$  planes. In contrast, the intensity of shoulder at approx. 932.9 eV is slightly increased with Eu doping, indicating slight more holes in the  $\text{CuO}_3$  ribbons. The depletion rate of hole carriers within the  $\text{CuO}_2$  planes in  $\text{Eu}(\text{Ba}_{1-x}\text{Pr}_x)_2\text{Cu}_3\text{O}_{7+\delta}$  is greater than that in  $\text{Eu}(\text{Ba}_{1-x}\text{Eu}_x)_2\text{Cu}_3\text{O}_{7+\delta}$ . Thus, the rate of  $T_c$  suppression in  $\text{Eu}(\text{Ba}_{1-x}\text{Pr}_x)_2\text{Cu}_3\text{O}_{7+\delta}$  with Pr doping is greater than that in  $\text{Eu}(\text{Ba}_{1-x}\text{Eu}_x)_2\text{Cu}_3\text{O}_{7+\delta}$  with Eu substitution. This rapid suppression of  $T_c$  is explained by partial substitution of Pr for Eu at the rare-earth site.

#### Acknowledgments

We thank the NSRRC staff for their technical support. This research is supported by the NSRRC and the National Science Council of the Republic of China under grants NSC 94-2113-M-213-001 and NSC-94-2113-M-002-030.

#### References

- [1] Soderholm L, Zhang K, Hinks D G, Beno M A, Jorgensen J D, Segre C U and Schuller I K 1987 *Nature (London)* **328** 604
- [2] Guan W Y, Xu Y H, Sheen S R, Chen Y C, Wei J Y T, Lai H F, Wu M K and Ho J C 1994 *Phys. Rev. B* **49** 15993
- [3] Matsui Y, Takekawa S and Iyi N 1987 *Japan. J. Appl. Phys.* **26** L1693
- [4] Li S, Hayri E A, Ramanujachary K V and Greenblatt M 1988 *Phys. Rev. B* **38** 2450
- [5] Xu Y, Kramer M J, Dennis K W, Wu H, O'Connor A, McCallum R W, Malik S K and Yelon W B 2000 *Physica C* **333** 195–206
- [6] Kramer M J, Dennis K W, Falzgraf D, McCallum R W, Malik S K and Yelon W B 1997 *Phys. Rev. B* **56** 5512
- [7] Zou Z, Oka K, Ito T and Nishihara Y 1997 *Japan. J. Appl. Phys.* **36** L18
- [8] Blackstead H A, Dow J D, Chrisey B, Horwitz J S, Black M A, McGinn P A, Klunzinger A E and Pulling D B 1996 *Phys. Rev. B* **54** 6122
- [9] Zou Z, Ye J, Oka K and Nishihara Y 1998 *Phys. Rev. Lett.* **80** 1074
- [10] Chen J M, Chang S C, Liu R S, Lee J M and Choy J H 2005 *Phys. Rev. B* **71** 094501
- [11] Nücker N, Pellegrin E, Schweiss P, Fink J, Molodtsov S L, Simmons C T, Kaindl G, Frentrup W, Erb A and Müller-Vogt G 1995 *Phys. Rev. B* **51** 8529

- [12] Zaanen J, Daxton A T, Jepsen O and Andersen O K 1988 *Phys. Rev. Lett.* **60** 2685
- [13] Merz M *et al* 1998 *Phys. Rev. Lett.* **80** 5192
- [14] Merz M *et al* 1997 *Phys. Rev. B* **55** 9160
- [15] Fink J, Nücker N, Pellegrin E, Romberg H, Alexander M and Knupfer M 1994 *J. Electron Spectrosc. Relat. Phenom.* **66** 395
- [16] Meinders M B J, Eskes H and Sawatzky G A 1993 *Phys. Rev. B* **48** 3916
- [17] Nücker N, Romberg H, Xi X X, Fink J, Gegenheimer B and Zhao Z X 1989 *Phys. Rev. B* **39** 6619
- [18] Chen J M, Liu R S, Chung S C, Liu R S, Kramer M J, Dennis K W and McCallum R W 1997 *Phys. Rev. B* **55** 3186
- [19] Chen J M, Liu S J, Chang C F, Lin J Y, Gou Y S and Yang H D 2003 *Phys. Rev. B* **67** 014502
- [20] Karppinen M, Kotiranta M, Nakane T, Chang S C, Chen J M, Liu R S and Yamauchi H 2003 *Phys. Rev. B* **67** 134522
- [21] Pellegrin E *et al* 1993 *Phys. Rev. B* **47** 3354
- [22] Schneider M, Unger R S, Mitdank R, Müller R, Krapf A, Rogaschewski S, Dwelk H, Janowitz C and Manzke R 2005 *Phys. Rev. B* **72** 014504
- [23] Tallon J L, Bernhard C, Shaked H, Hitterman R L and Jorgensen J D 1995 *Phys. Rev. B* **51** 12911
- [24] Klencsar Z, Kuamann E, Homonnay A, Vertes A, Vad K, Bankuti J, Racz, T, Bodog M and Kotsis I 1998 *Physica C* **304** 124